Advances in Aircraft and Spacecraft Science, *Vol. 4, No. 3 (2017) 269-280*
DOI: http://dx.doi.org/10.12989/aas.2017.4.3.269

Vibration analysis of generalized thermoelastic microbeams resting on visco-Pasternak's foundations

Ashraf M. Zenkour*[1,2]

[1]*Department of Mathematics, Faculty of Science, King Abdulaziz University, Jeddah 21589, Saudi Arabia*
[2]*Department of Mathematics, Faculty of Science, Kafrelsheikh University, Kafrelsheikh 33516, Egypt*

(Received March 10, 2016, Revised June 28, 2016, Accepted July 22, 2016)

Abstract. The natural vibration analysis of microbeams resting on visco-Pasternak's foundation is presented. The thermoelasticity theory of Green and Naghdi without energy dissipation as well as the classical Euler-Bernoulli's beam theory is used for description of natural frequencies of the microbeam. The generalized thermoelasticity model is used to obtain the free vibration frequencies due to the coupling equations of a simply-supported microbeam resting on the three-parameter viscoelastic foundation. The fundamental frequencies are evaluated in terms of length-to-thickness ratio, width-to-thickness ratio and three foundation parameters. Sample natural frequencies are tabulated and plotted for sensing the effect of all used parameters and to investigate the visco-Pasternak's parameters for future comparisons.

Keywords: thermoelasticity theory; microbeam; vibration frequencies; viscoelastic foundations

1. Introduction

The analysis of beams is one of important topics in civil engineering, and it was a subject of investigation for many decades. Vibrations of the beam-structured resting on elastic foundations are of a wide practical interest involving applications such as analyses of roads, rail tracks and foundations of diverse structures. There have been a large number of publications related to this problem considering different types of foundation such as Winkler, Pasternak, elastic or visco-elastic, linear or non-linear. The Winkler's foundation parameter is capable of just normal load while Pasternak's foundation parameter is both capable of transverse shear and normal loads. The influence of the viscosity or damping as a third parameter of the foundation is still very rare in the literature. In last decades, the dynamic response analysis of such beams on thermo-visco-elastic foundation has been one of the research interests of many engineering applications. So far and during these years many researchers have conducted and investigated different studies in this field.

The simple viscoelastic foundation model is consisting of a spring of constant stiffness and a dashpot of viscosity coefficient that placed parallel (visco-Winkler's foundation model). Sun (2001) has used Fourier's transform to solve the problem of steady state response of a beam on a viscoelastic foundation subjected to a harmonic line load. Chen *et al.* (2001) have established the dynamic stiffness matrix of beams on viscoelastic foundations subjected to a harmonic moving

*Corresponding author, Professor, E-mail: zenkour@kau.edu.sa

http://www.techno-press.org/?journal=aas&subpage=7 ISSN: 2287-528X (Print), 2287-5271 (Online)

load as a function of the velocity and frequency of the harmonic moving load. Ding *et al.* (2012) have introduced an investigation of the convergence of the Galerkin's method for the dynamic response of a uniform beam resting on a nonlinear foundation with viscous damping subjected to a moving concentrated load. The foundation is taken as a nonlinear Winkler's foundation with linear-plus-cubic stiffness and viscous damping with three parameters. Jumel *et al.* (2013) have presented the Winkler's viscoelastic foundation analysis of single cantilevered beam under stationary loading.

The dynamic response of beams on the generalized Pasternak's viscoelastic foundations subjected to an arbitrary distributed harmonic moving load has been analyzed in Kargarnovin and Younesian (2004). Kargarnovin *et al.* (2005) have studied the response of infinite beams supported by nonlinear viscoelastic foundation subjected to harmonic moving loads. They have solved the governing equations using perturbation method in conjunction with complex Fourier's transformation. Younesian *et al.* (2006) have studied the vibration response of a Timoshenko beam supported by a viscoelastic foundation with randomly distributed parameters along the beam length. They have assumed that the beam is subjected to a harmonic moving load by employing appropriate Green's functions. Muscolino and Palmeri (2007) have presented the response of beams resting on viscoelastic damped foundation under moving oscillators. Sapountzakis and Kampitsis (2011) have developed a boundary element method for the geometrically nonlinear response of shear deformable beams of simply or multiply connected constant cross-section. These beams may be traversed by moving loads and resting on tensionless nonlinear three-parameter viscoelastic foundation. Zhang and Wang (2012) have presented the interface stress redistribution in FRP-strengthened reinforced concrete beams using a three-parameter viscoelastic foundation model. Goodarzi *et al.* (2014) have studied the free vibration behavior of rectangular graphene sheet under visco-Pasternak's foundation using the nonlocal elasticity. Mohammadimehr *et al.* (2015) have investigated the free vibration analysis of tapered viscoelastic micro-rod resting on visco-Pasternak's foundation based on strain gradient theory. Hashemi *et al.* (2015) have presented the exact solution for free vibration of coupled double viscoelastic graphene sheets by visco-Pasternak's medium based on the nonlocal theory. Peng and Wang (2015) have investigated the transverse vibration frequencies of finite Euler-Bernoulli's beams resting on three-parameter viscoelastic foundations using differential quadrature method.

The vibration problem of elastic structures resting on viscoelastic foundation displays viscous characters, and the solution becomes difficult. The author has presented some publications on the topic of finite structures resting on elastic foundation (Zenkour 2009, 2010, 2015, Zenkour and Sobhy 2011, Al Khateeb and Zenkour 2014), the foundation is assumed as linear elastic one, or two, and the problems are mainly studied. Recently, Zenkour (2016a, b) has presented nonlocal transient thermal analysis of a single-layered graphene sheet embedded in visco-Pasternak's medium using nonlocal elasticity theory.

Wide applications of micro-mechanical system in different industrial fields such as biomedical engineering, aviation and aerospace industries have convinced many researchers to focus on the analysis of vibration of microstructures such as microbeams and microplates. Since, when thickness of plate decreases and reaches to the order of microns, the size-effect plays an important role in the mechanical behaviors of microplates. In most literature, the vibration problems of thermal microbeam embedded with elastic or viscoelastic medium are solved by using a simple classical or shear deformation theories with appropriate boundary conditions. The inclusion of the thermal effect has been considered without solving the heat conduction equation. With respect to developmental works on analysis of coupled thermoelasticity, it should be noted that none of the

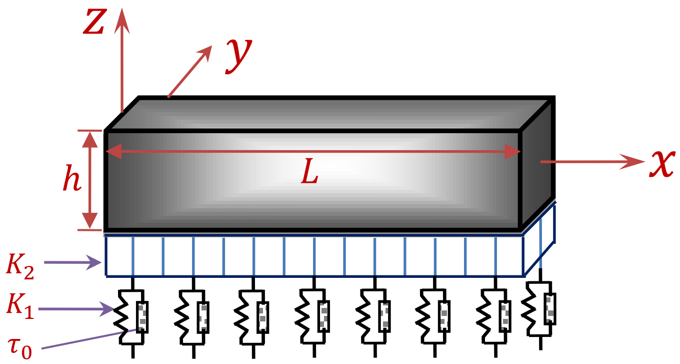

Fig. 1 Schematic diagram for the microbeam resting on visco-Pasternak's foundations

research mentioned above or in the literature, has considered such coupled thermoelasticity problem.

The present paper deals with the dynamic response of generalized thermoelastic microbeam resting on three-parameter elastic foundation. The microbeam is embedded with three-parameter viscoelastic medium where simulated by visco-Pasternak's type as spring, shear and damping foundations. The heat conduction in the context of Green and Naghdi's generalized thermoelasticity theory without energy dissipation is considered. The coupled differential equations are used to get the natural vibration frequencies. The effects of many parameters on the vibration frequencies are investigated. Various results are graphically illustrated and sample results are tabulated for future comparisons.

2. The GN thermoelastic and Euler-Bernoulli model

Let us consider a rectangular microbeam (Fig. 1) of length $L\,(0 \le x \le L)$, width $b\,(-b/2 \le y \le b/2)$ and thickness $h\,(-h/2 \le z \le h/2)$ with cross-section of area $A = hb$. We define the x-coordinate along the axis of the beam, with the y- and z- coordinates corresponding to the width and thickness, respectively. The beam is made of a homogeneous isotropic and linearly elastic material with modulus of elasticity E and Poisson's ratio ν. The beam is supported on a homogeneous three-parameter viscoelastic soil. The foundation model is characterized by the linear Winkler's modulus K_1, the Pasternak's (shear) foundation modulus K_2 and the damping coefficient τ_0. Taking into account the un-bonded contact between beam and soil, the interaction between the beam and the supporting foundation can be only compressive and follows the three-parameter Pasternak's model as

$$R_f = K_1 w(x,t) - K_2 \frac{\partial^2 w}{\partial x^2} - \tau_0 \frac{\partial w}{\partial t}, \tag{1}$$

where R_f is the foundation reaction per unit area, w is the lateral deflection and τ_0 may said to be the mechanical relaxation time due to the viscosity. This model is simply reducing to the visco-Winkler's type when $K_2 = 0$. The viscosity term may be omitted by setting $\tau_0 = 0$ to get the thermoelastic analysis of the microbeam on simple elastic foundation.

In equilibrium, the beam is unstrained, at zero stress and constant temperature T_0 everywhere. The beam undergoes bending vibrations of small amplitude about the x-axis such that the deflection is consistent with the linear Euler-Bernoulli's (E-B) theory. That is, any plane cross-section initially perpendicular to the axis of the beam remains plane and perpendicular to the neutral surface during bending. Thus, the displacements are given by

$$u = -z\frac{\partial w}{\partial x}, \quad v = 0, \quad w = w(x,t), \tag{2}$$

The time-dependency is considered in entire displacement components u and w. The relevant constitutive equation for the axial stress σ_x reads

$$\sigma_x = -E\left(z\frac{\partial^2 w}{\partial x^2} + \alpha_T\theta\right), \tag{3}$$

where $\theta = T - T_0$ is the excess temperature with T_0 denoting the constant environmental temperature, $\alpha_T = \alpha_t/(1-2\nu)$ in which α_t is the thermal expansion coefficient.

For transverse deflections, the corresponding equation of motion reads

$$\frac{\partial^2 M}{\partial x^2} - R_f = \rho A\ddot{w}, \tag{4}$$

where ρ is the material density and the superimposed dot indicates partial derivative with respect to time t. Accordingly, the E-B flexural moment of the cross-section is given, with aid of Eq. (3), by the expression

$$M = -EI\left(\frac{\partial^2 w}{\partial x^2} + \alpha_T M_T\right), \tag{5}$$

where $I = bh^3/12$ is the moment of inertia, EI is the flexural rigidity of the beam, and M_T is the thermal moment defined by

$$M_T = \frac{12}{h^3}\int_{-h/2}^{h/2} \theta(x,z,t)z\mathrm{d}z. \tag{6}$$

Substituting Eqs. (1) and (5) into Eq. (4), one obtains the motion equation of the beam in the form

$$\left(\frac{\partial^4}{\partial x^4} - \frac{K_2}{EI}\frac{\partial^2}{\partial x^2} + \frac{\rho A}{EI}\frac{\partial^2}{\partial t^2} - \frac{\tau_0}{EI}\frac{\partial}{\partial t} + \frac{K_1}{EI}\right)w + \alpha_T\frac{\partial^2 M_T}{\partial x^2} = 0. \tag{7}$$

The heat conduction in the context of Green and Naghdi's generalized thermoelasticity theory without energy dissipation is given by (Green and Naghdi 1993)

$$\kappa^*\nabla^2\theta + \left(1 + \frac{\partial}{\partial t}\right)(\rho Q^*) = \frac{\partial}{\partial t}\left(\rho C^v\frac{\partial\theta}{\partial t} + \gamma T_0\frac{\partial e}{\partial t}\right), \tag{8}$$

where κ^* is the thermal conductivity (the material constant characteristic), C^v is the specific heat per unit mass at constant strain, $e = \varepsilon_{kk} = \frac{\partial u}{\partial x} + \frac{\partial v}{\partial y} + \frac{\partial w}{\partial z}$ is the volumetric strain, Q^* is the heat source, and $\gamma = \alpha_T E = \alpha_t E/(1-2\nu)$ is the thermoelastic coupling parameter. The corresponding thermal conduction equation for the microbeam under consideration without heat source is obtained by specializing Eq. (8) to present the E-B beam configuration as

$$\frac{\partial^2\theta}{\partial x^2} + \frac{\partial^2\theta}{\partial z^2} = \frac{1}{\kappa^*}\frac{\partial^2}{\partial t^2}\left(\rho C^v\theta - \gamma T_0 z\frac{\partial^2 w}{\partial x^2}\right). \tag{9}$$

Multiplying Eq. (9) by $\frac{12z}{h^3}$, and integrating it with respect to z through the beam thickness from $-\frac{h}{2}$ to $\frac{h}{2}$, yields

$$\frac{\partial^2 M_T}{\partial x^2} + z\frac{\partial\theta}{\partial z}\Big|_{-h/2}^{+h/2} - \frac{12}{h^3}\theta\Big|_{-\frac{h}{2}}^{+\frac{h}{2}} = \frac{1}{\kappa^*}\frac{\partial^2}{\partial t^2}\left(\rho C^v M_T - \gamma T_0\frac{\partial^2 w}{\partial x^2}\right). \tag{10}$$

Since no heat flow occurs across the upper and lower surfaces of the beam (thermally insulated), it follows that $\frac{\partial\theta}{\partial z}\Big|_{-h/2}^{+h/2} = 0$. For the present microbeam, it is assumed that there is a cubic polynomial variation of temperature increment along the thickness direction. This assumption leads to (Guo and Rogerson 2003)

$$M_T = \frac{6}{5h}\theta\Big|_{-h/2}^{+h/2}. \tag{11}$$

So, at this point Eq. (10) becomes

$$\frac{\partial^2 M_T}{\partial x^2} - \frac{10}{h^2}M_T = \eta\frac{\partial^2}{\partial t^2}\left(M_T - \frac{\varepsilon}{\alpha_T}\frac{\partial^2 w}{\partial x^2}\right), \tag{12}$$

where $\varepsilon = \frac{\alpha_T\gamma T_0}{\eta\kappa^*}$ and $\eta = \frac{\rho C^v}{\kappa^*}$.

3. Analytical solution

We now search for analytical solutions of the coupled system of Eqs. (7) and (12), along with Eq. (5) for the bending moment. Concerning the heat conditions of the present microbeam, we assume that no heat flow occurs across its upper and lower surfaces (thermally insulated), that is

$$\frac{\partial\theta}{\partial z}\Big|_{z=\pm h/2} = 0. \tag{13}$$

However, the microbeam is subjected to simply-supported mechanical conditions at its edges $x = 0$ and $x = L$ as

$$w = M = 0. \tag{14}$$

Following the Navier-type solution, the deflection and moment that satisfy the boundary conditions may be expressed as

$$\{w(x,t), M(x,t)\} = \sum_{n=1}^{N}\{w_n^*, M_n^*\}\sin(\lambda_n x)\,\mathrm{e}^{\omega t}, \tag{15}$$

where w_n^* and M_n^* are arbitrary parameters, $\lambda_n = \frac{n\pi}{L}$, n is a mode number and ω denotes the complex angular frequency. According to Eqs. (5) and (13), the thermal bending moment has the same behavior form as the bending moment. Substituting Eq. (15) into Eqs. (7) and (12) gives

$$\left(\lambda_n^4 + \frac{K_1}{EI} + \frac{K_2}{EI}\lambda_n^2 - \frac{\tau_0}{EI}\omega + \frac{\rho A}{EI}\omega^2\right)w_n^* - \alpha_T\lambda_n^2 M_{nT}^* = 0, \tag{16}$$

$$\eta\varepsilon\lambda_n^2\omega^2 w_n^* + \alpha_T\left(\eta\omega^2 + \lambda_n^2 + \frac{10}{h^2}\right)M_{nT}^* = 0. \tag{17}$$

where M_{nT}^* is an arbitrary thermal parameter.

The angular frequency is given in the form $\omega = \omega_0 + i\zeta$ where i is an imaginary unit. Then $\mathrm{e}^{\omega t} = \mathrm{e}^{\omega_0 t}(\cos\zeta t + i\sin\zeta t)$ and for small values of time, most investigators may take the real value of ω (i.e., $\omega = \omega_0$). Here, we will get the fundamental frequencies for the present beam with and without the inclusion of ζ. In what follows we will use the following dimensionless variables

$$\{\acute{\omega}, \acute{\omega}_0, \acute{\zeta}\} = \frac{L^2}{h}\sqrt{\frac{\rho}{E}}\{\omega, \omega_0, \zeta\}, \quad \acute{\tau}_0 = \frac{h}{L^2}\sqrt{\frac{E}{\rho}}\tau_0. \tag{18}$$

Then, the governing equations, Eqs. (16) and (17) become (dropping the acute sign for convenience)

$$\left[h^4\lambda_n^4 + k_1 + h^2\lambda_n^2 k_2 - \frac{12h\tau_0}{Eb}(\omega_0 + i\zeta) + \frac{12h^4}{L^4}(\omega_0 + i\zeta)^2\right] w_n^* - \alpha_T h^4 \lambda_n^2 M_{nT}^* = 0, \tag{19}$$

$$\eta\varepsilon E h^2\lambda_n^2(\omega_0 + i\zeta)^2 w_n^* + \alpha_T\left[\eta E h^2(\omega_0 + i\zeta)^2 + \rho L^4\left(\lambda_n^2 + \frac{10}{h^2}\right)\right] M_{nT}^* = 0, \tag{20}$$

where $k_1 = \frac{h^4 K_1}{EI}$ and $k_2 = \frac{h^2 K_2}{EI}$ are the dimensionless foundation parameters. To get the nontrivial solution of the above equations, the parameter w_n^* and M_{nT}^* must be nonzero. Then, the determinate of the coefficients should be vanished. This tends to the frequency equation

$$\omega^4 - A_3\omega^3 + A_2\omega^2 - A_1\omega + A_0 = 0, \tag{21}$$

where

$$\begin{aligned} A_0 &= \frac{\rho}{12\eta E}\left[h_L^6\bar{\lambda}_n^6 + (k_2 + 10)h_L^4\bar{\lambda}_n^4 + (k_1 + 10k_2)h_L^2\bar{\lambda}_n^2 + 10k_1\right], \quad A_3 = \frac{h_b\tau_0}{h_L^4 E}, \\ A_1 &= \frac{\rho h_b \tau_0}{\eta E^2 h_L^8}\left(h_L^2\bar{\lambda}_n^2 + 10\right), \quad A_2 = \frac{1}{12}\left(1 + \frac{\varepsilon}{\eta}\right)\bar{\lambda}_n^4 + \frac{k_1}{12h_L^4} + \frac{\bar{\lambda}_n^2 k_2}{12h_L^2} + \frac{\rho}{\eta E h_L^2}\left(\bar{\lambda}_n^2 + \frac{10}{h_L^2}\right), \end{aligned} \tag{22}$$

in which $h_L = \frac{h}{L}$, $h_b = \frac{h}{b}$ and $\bar{\lambda}_n = n\pi$. If we neglect ζ, the frequency equation is given as in Eq. (21) with ω tends ω_0. However, the frequency equation with the inclusion of ζ is given by

$$\omega_0^4 - B_3\omega_0^3 + B_2\omega_0^2 - B_1\omega_0 + B_0 = 0, \tag{23}$$

where

$$\begin{aligned} B_0 &= A_0 + \zeta^4 + iA_3\zeta^3 - A_2\zeta^2 - iA_1\zeta, \\ B_1 &= A_1 + 4i\zeta^3 - 3A_3\zeta^2 - 2iA_2\zeta, \quad B_2 = A_2 - 6\zeta^2 - 3iA_3\zeta, \quad B_3 = A_3 - 4i\zeta. \end{aligned} \tag{24}$$

The four roots of Eq. (23) are given by

$$\frac{1}{4}B_3 + \frac{\xi^2 \pm \sqrt{-\xi^4 - 2\xi^2 c_2 - 2\xi c_1}}{2\xi}, \quad \frac{1}{4}B_3 - \frac{\xi^2 \pm \sqrt{-\xi^4 - 2\xi^2 c_2 + 2\xi c_1}}{2\xi}, \tag{25}$$

where $\xi^2 = 2\bar{\xi} - c_2$ and $\bar{\xi}$ is the real root of the equation

$$\bar{\xi}^3 - \frac{1}{2}c_2\bar{\xi}^2 - c_0\bar{\xi} + \frac{1}{2}c_0 c_2 - \frac{1}{8}c_1^2 = 0, \tag{26}$$

in which

$$\begin{aligned} c_0 &= B_0 - \frac{1}{4}B_1 B_3 + \frac{1}{16}B_2 B_3^2 - \frac{3}{256}B_3^4, \\ c_1 &= -B_1 + \frac{1}{2}B_2 B_3 - \frac{1}{8}B_3^3, \quad c_2 = B_2 - \frac{3}{8}B_3^2. \end{aligned} \tag{27}$$

4. Numerical results and discussions

Let us consider several numerical applications to put into evidence the influence of the length-to-thickness ratio, the width-to-thickness ratio, the foundation parameters, and the viscous damping coefficient. The material used for the present microbeam is the silicon at reference temperature $T_0 = 293$ K with the following properties (Sun and Saka 2010)

$$E = 165.9 \text{ GPa}, \quad \nu = 0.22, \quad \rho = 2330 \text{ kg/m}^3, \\ C^v = 1.661 \text{ J/kg K}, \quad \alpha_T = 2.59\ (10^{-6}/\text{K}), \quad \kappa^* = 156 \text{ W/mK}. \tag{28}$$

All plots are prepared by using the smallest real value of the dimensionless parameter ω_0. The imaginary part ζ has a very trivial effect and so it may be neglected. Reliable fundamental frequency $(n = 1)$ and natural frequencies $(n > 1)$ are graphically illustrated. The computations are carried out (except otherwise stated) for $L/h = 10$, $b/h = 1$, $k_1 = 0.05$, and $k_2 = 0.1$. Other different values are given to the visco-Pasternak's parameters τ_0, k_1, and k_2 and the length-to-thickness ratio L/h.

Benchmark results are presented in Table 1 for future comparisons with other investigators. The effect of visco-Pasternak's parameters on the free natural frequencies is discussed. It is to be noted that the natural vibration frequency ω_0 increases as n, k_1, and k_2 increase. However ω_0 decreases as τ_0 increases.

Figs. 2 and 3 show the fundamental frequency ω_0 vs the viscous damping coefficient τ_0 for various foundation parameters with $L/h = 10$ and $L/h = 20$, respectively. The fundamental frequency is increasing to a maximum vertex point then it is rapidly decreasing again. The path in which ω_0 increases is the same for different foundation parameters. The position of the maximum vertex point is rising with the increase of the foundation parameter. The two plots show the sensitivity of ω_0 to the variation of viscous damping coefficient τ_0.

Table 1 Effect of the viscous damping coefficient τ_0 and the foundation parameters k_1 and k_2 on the natural frequency ω_0

τ_0	k_1	k_2	n				
			1	2	3	4	5
0.5	0	0	0.05322	0.85604	4.43850	15.11765	48.96565
	0.05	0.1	1.57321	2.76914	7.11527	19.41279	67.74684
	0.1	0.2	3.12477	4.73337	9.89988	24.05997	76.28843
	0.2	0.3	6.19891	8.28674	14.49026	31.45709	76.28995
0.7	0	0	0.03801	0.60977	3.12381	10.21710	27.21950
	0.05	0.1	1.11799	1.96004	4.96052	12.87848	31.57026
	0.1	0.2	2.20911	3.32794	6.83097	15.61751	36.18857
	0.2	0.3	4.33591	5.75254	9.81854	19.64316	42.75696
1.0	0	0	0.02660	0.42621	2.17012	6.96904	17.64611
	0.05	0.1	0.78049	1.36555	3.43029	8.72064	20.16563
	0.1	0.2	1.53814	2.31076	4.70119	10.49383	22.73404
	0.2	0.3	3.00308	3.96999	6.70435	13.04327	26.18602
1.5	0	0	0.01773	0.28392	1.44100	4.58587	11.36602
	0.05	0.1	0.51959	0.90810	2.27243	5.71907	12.92003
	0.1	0.2	1.02254	1.53398	3.10693	6.85806	14.48530
	0.2	0.3	1.99101	2.62730	4.41393	8.48098	16.55828

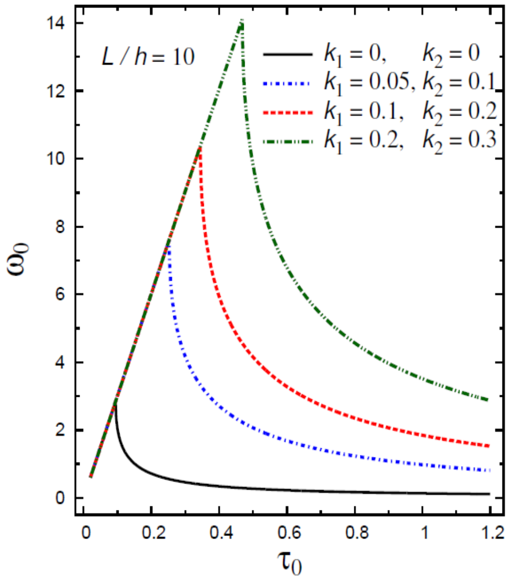

Fig. 2 The fundamental frequency ω_0 vs the viscous damping coefficient τ_0 for various foundation ($L/h = 10$)

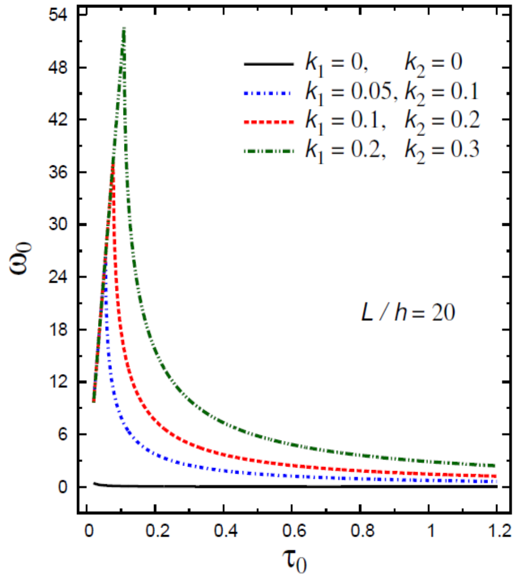

Fig. 3 The fundamental frequency ω_0 vs the viscous damping coefficient τ_0 for various foundation ($L/h = 20$)

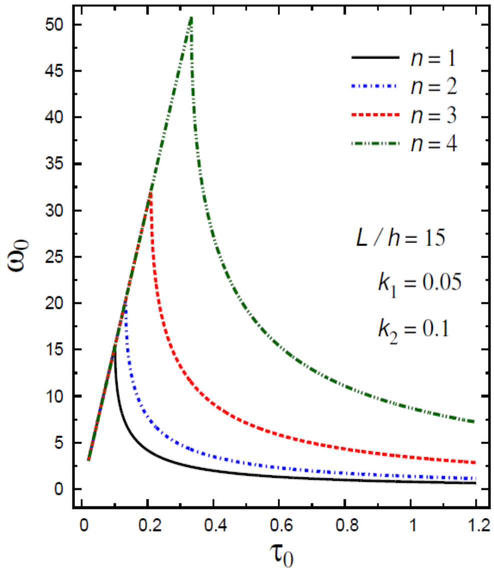

Fig. 4 The natural frequency ω_0 vs the viscous damping coefficient τ_0

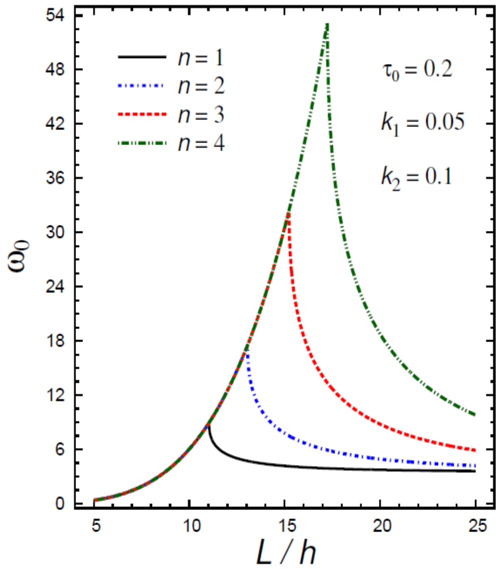

Fig. 5 The natural frequency ω_0 vs the length-to-thickness ratio L/h

The natural frequency ω_0 vs the viscous damping coefficient τ_0 is plotted in Fig. 4. Once again, ω_0 increases to a maximum vertex point then it is rapidly decreasing again. The path in which ω_0 increases is the same for different modes n. The position of the maximum vertex point is rising with the increase of the mode n. Fig. 5 shows the natural frequency ω_0 vs the length-to-

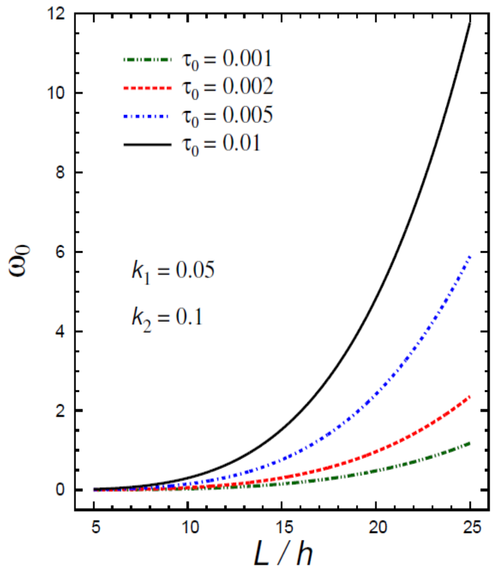

Fig. 6 The fundamental frequency ω_0 vs the length-to-thickness ratio L/h for smaller values of the viscous damping coefficient τ_0

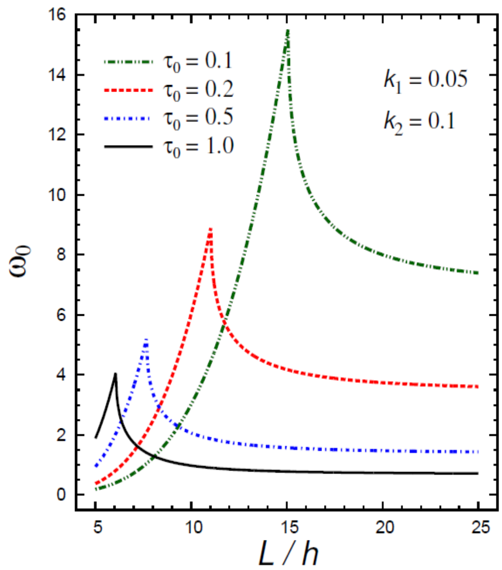

Fig. 7 The fundamental frequency ω_0 vs the length-to-thickness ratio L/h for greater values of the viscous damping coefficient τ_0

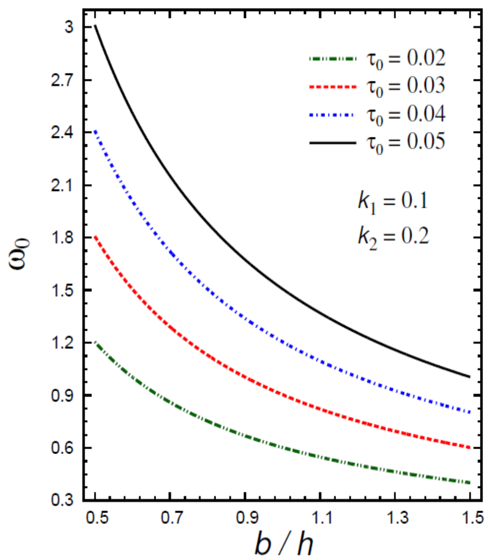

Fig. 8 The fundamental frequency ω_0 vs the width-to-thickness ratio b/h for smaller values of the viscous damping coefficient τ_0

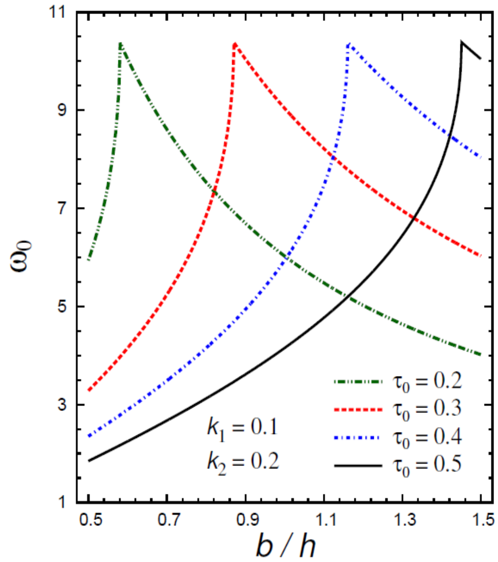

Fig. 9 The fundamental frequency ω_0 vs the width-to-thickness ratio b/h for greater values of the viscous damping coefficient τ_0

thickness ratio L/h. Also, ω_0 increases to a maximum vertex point then it is rapidly decreasing again. The path in which ω_0 increases is the same for different modes n. The position of the maximum vertex point is rising with the increase of the mode n and ω_0 is sensitive to the variation of L/h ratio.

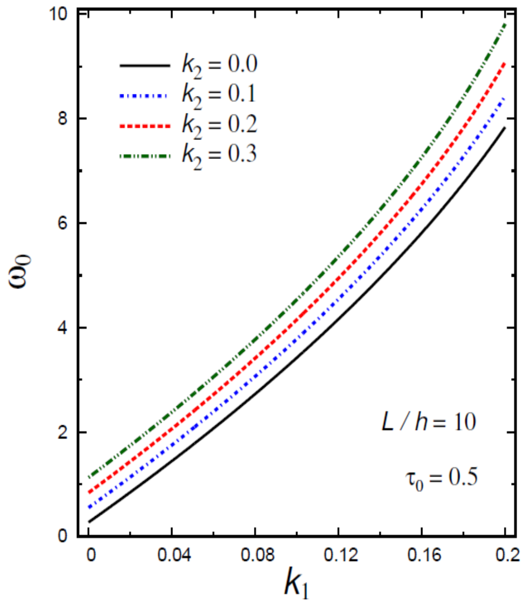

Fig. 10 The fundamental frequency ω_0 vs the Winkler's parameter k_1 for different values of the Pasternak's parameter k_2

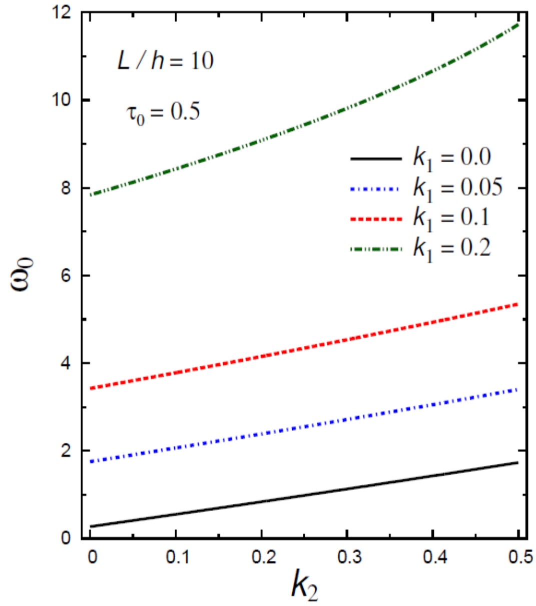

Fig. 11 The fundamental frequency ω_0 vs the Pasternak's parameter k_2 for different values of the Winkler's parameter k_1

In Figs. 6 and 7, the fundamental frequency ω_0 is plotted vs the length-to-thickness ratio L/h for smaller and greater values of the viscous damping coefficient τ_0, respectively. For small values of the viscous damping coefficient τ_0, the fundamental frequency ω_0 increases as L/h increases. The greatest value of τ_0 always gives the highest frequency ω_0. However, for high values of τ_0 the fundamental frequency increases to get its maximum vertex then it is rapidly decreasing. Different paths to the vertex points occur according to the value of the viscous damping coefficient τ_0 and the length-to-thickness ratio L/h. Here, the smallest value of τ_0 always gives the highest frequency ω_0.

The fundamental frequency ω_0 vs the width-to-thickness ratio b/h for smaller and greater values of the viscous damping coefficient τ_0 is plotted in Figs. 8 and 9, respectively. For small values of the viscous damping coefficient τ_0, the fundamental frequency ω_0 decreases as b/h increases and as τ_0 decreases. However, for high values of τ_0 the fundamental frequency increases to get its maximum vertex then it is rapidly decreasing. Different paths to the vertex points occur according to the value of the viscous damping coefficient τ_0 and the width-to-thickness ratio b/h. It is interesting here to notice that the maximum vertex points are at the same level of height.

In Figs. 10 and 11, the length-to-thickness ratio and the viscous damping coefficient are kept fixed as $L/h = 10$ and $\tau_0 = 0.5$. Fig. 10 shows that the frequency increases as the first foundation Winkler's parameter k_1 increases. The same behavior occurs in Fig. 11 that ω_0 increases as the second foundation Pasternak's parameter k_2 increases. In contrast, the dimensionless natural frequency depends upon the length- or width-to-thickness ratio and the two-parameter elastic foundation as well as the viscous damping coefficient.

5. Conclusions

In this article, a novel three-parameter viscoelastic foundation model is proposed to study the visco-Pasternak's elastic behavior of the generalized thermoelastic microbeams. The vibration frequency analysis is performed and the effects of length-to-thickness ratio, width-to-thickness ratio, and the three-parameter viscoelastic foundation have been evaluated on the free vibration of the microbeam. The parameters of foundation, especially the viscous damping coefficient, have considerable effect on the dynamic responses of the microbeam. The obtained results indicate that with increasing the Winkler's and shear parameters of foundation, the frequencies of the microbeam are increased. This increasing is due to increasing the stiffness of the beam. However, the increase of the viscous damping coefficient tends to decreasing of the frequencies. For the sake of completeness and comparisons, some natural frequencies are tabulated here for different viscous damping coefficient and two-parameter elastic foundation. The inclusion of the thermoelastic coupling effect is required to get reliable frequencies.

References

Al Khateeb, S.A. and Zenkour, A.M. (2014), "A refined four-unknown plate theory for advanced plates resting on elastic foundations in hygrothermal environment", *Compos. Struct*., **111**(1), 240-248.

Chen, Y.H., Huang, Y.H. and Shih, C.T. (2001), "Response of an infinite Timoshenko beam on a viscoelastic foundation to a harmonic moving load", *J. Sound Vib.*, **241**, 809-824.

Ding, H., Chen, L.Q. and Yang, S.P. (2012), "Convergence of Galerkin truncation for dynamic response of finite beams on nonlinear foundations under a moving load", *J. Sound Vib.*, **331**, 2426-2442.

Goodarzi, M., Mohammadi, M., Farajpour, A. and Khooran, M. (2014), "Investigation of the effect of pre-stressed on vibration frequency of rectangular nanoplate based on a viscoPasternak foundation", *J. Solid Mech.*, **6**, 98-121.

Green, A.E. and Naghdi, P.M. (1993), "Thermoelasticity without energy dissipation", *J. Elast.*, **31**, 189-208.

Guo, F.L. and Rogerson, G.A. (2003), "Thermoelastic coupling effect on a micro-machined beam resonator", *Mech. Res. Commun.*, **30**, 513-518.

Hashemi, S.H., Mehrabani, H. and Ahmadi-Savadkoohi, A. (2015), "Exact solution for free vibration of coupled double viscoelastic graphene sheets by viscoPasternak medium", *Composit. B*, **78**, 377-383.

Jumel, J., Chauffaille, S., Budzik, M.K., Shanahan, M.E.R. and Guitard, J. (2013), "Viscoelastic foundation analysis of single cantilevered beam (SCB) test under stationary loading", *Eur. J. Mech. A/Solid*., **39**, 170-179.

Kargarnovin, M.H. and Younesian, D. (2004), "Dynamics of timoshenko beams on Pasternak foundation under moving load", *Mech. Res. Commun.*, **31**, 713-723.

Kargarnovin, M.H., Younesian, D., Thompson, D. and Jones, C. (2005), "Response of beams on nonlinear viscoelastic foundations to harmonic moving loads", *Comput. Struct.*, **83**, 1865-1877.

Mohammadimehr, M., Monajemi, A.A. and Moradi, M. (2015), "Vibration analysis of viscoelastic tapered micro-rod based on strain gradient theory resting on visco-Pasternak foundation using DQM", *J. Mech. Sci. Tech.*, **29**, 2297-2305.

Muscolino, G. and Palmeri, A. (2007), "Response of beams resting on viscoelastically damped foundation to moving oscillators", *Int. J. Solid. Struct.*, **44**, 1317-1336.

Peng, L. and Wang, Y. (2015), "Free vibrations of beams on viscoelastic Pasternak foundations", *Appl. Mech. Mater.*, **744-746**, 1624-1627.

Sapountzakis, E.J. and Kampitsis, A.E. (2011), "Nonlinear response of shear deformable beams on tensionless nonlinear viscoelastic foundation under moving loads", *J. Sound Vib.*, **330**, 5410-5426.

Sun, L. (2001), "A closed-form solution of a Bernoulli-Euler beam on a viscoelastic foundation under

harmonic line loads”, *J. Sound Vib.*, **242**, 619-627.
Sun, Y. and Saka, M. (2010), “Thermoelastic damping in micro-scale circular plate resonators”, *J. Sound Vib.*, **329**, 328-337.
Younesian, D., Kargarnovin, M., Thompson, D. and Jones, C. (2006), “Parametrically excited vibration of a Timoshenko beam on random viscoelastic foundation subjected to a harmonic moving load”, *Nonlin. Dyn.*, **45**, 75-93.
Zenkour, A.M. (2009), “The refined sinusoidal theory for FGM plates resting on elastic foundations”, *Int. J. Mech. Sci.*, **51**, 869-880.
Zenkour, A.M. (2010), “Hygro-thermo-mechanical effects on FGM plates resting on elastic foundations”, *Compos. Struct.*, **93**, 234-238.
Zenkour, A.M. (2015), “A comparative study for bending of composite laminates resting on elastic foundations”, *Smart Struct. Syst.*, **15**, 1569-1582.
Zenkour, A.M. (2016a), “Nonlocal transient thermal analysis of a single-layered graphene sheet embedded in viscoelastic medium”, *Physica E.*, **79**, 87-97.
Zenkour, A.M. (2016b), “Vibration analysis of a single-layered graphene sheet embedded in visco-Pasternak’s medium using nonlocal elasticity theory”, *J. Vibroeng.*, **18**, 2319-2330.
Zenkour, A.M. and Sobhy, M. (2011), “Thermal buckling of functionally graded plates resting on elastic foundations using the trigonometric theory”, *J. Therm. Stress.*, **34**, 1119-1138.
Zhang, C. and Wang, J. (2012), “Interface stress redistribution in FRP-strengthened reinforced concrete beams using a three-parameter viscoelastic foundation model”, *Compos. B*, **43**, 3009-3019.

EC